

Galaxy Zoo: Investigating the Star Formation History of the Green Valley

R. J. Smethurst,¹ C. J. Lintott,^{1,2} B. D. Simmons,¹ K. Schawinski,³ K. L. Masters,⁴

¹ Oxford Astrophysics, Department of Physics, University of Oxford, Denys Wilkinson Building, Keble Road, Oxford, OX1 3RH, UK

² Adler Planetarium, 1300 S Lake Shore Drive, Chicago, IL, 60605, USA

³ Institute for Astronomy, Department of Physics, ETH Zurich, Wolfgang-Pauli Strasse 27, CH-8093 Zurich, Switzerland

⁴ Institute of Cosmology and Gravitation, University of Portsmouth, Dennis Sciama Building, Barnaby Road, Portsmouth, PO1 3FX, UK

5 May 2014

ABSTRACT

Does galactic evolution proceed through the Green Valley via multiple pathways or as a single population? Motivated by recent results which used a toy model to highlight radically different evolutionary pathways between early- and late-type galaxies, we present results from an advanced Bayesian approach to this problem wherein we model the star formation history of a galaxy and compare the predicted and observed optical and near-ultraviolet colours in the model parameter space. We investigate the most probable values for these parameters for both disc-like and elliptical-like populations of galaxies, incorporating the morphological vote fractions from Galaxy Zoo^{*} into our analysis. We will discuss the implications of our results on the understanding of the simultaneous morphological-colour evolution of galaxies, particularly of those residing in the Green Valley.

1 INTRODUCTION

The Green Valley galaxies occupy a low density area of the colour-magnitude diagram between the *red sequence* and *blue cloud*. How they came to be there and why there are relatively so few of them has been a source of debate for many years (*cite lots of people here*).

WHAT is the green valley?

WHY do we think quenching is important?

WHAT is causing this quenching?

WHY do we care?

WHAT is our motivation?

WHAT are we going to do about it that's different?

A previous Galaxy Zoo investigation by Schawinski et al. (2014), found two contrastingly different evolutionary pathways between morphological types across the Green Valley by using a toy model; this study will expand on this by providing a full Bayesian analysis of this problem.

In this investigation we aim to determine:

- (i) What previous star formation history (SFH) causes a galaxy to reside in the green valley at the current epoch?
- (ii) Is the green valley a transitional or static population?
- (iii) If the green valley is a transitional population then how many routes through it are there?

* This investigation has been made possible by the participation of more than 250,000 volunteers in the Galaxy Zoo project. Their contributions are individually acknowledged at <http://www.galaxyzoo.org/volunteers.aspx>

- (iv) Are there morphological dependant differences between these routes through the green valley?

- (v) What previous SFHs allow for the composition of the colour-magnitude diagram at the current epoch?

This paper proceeds as follows. Section 2 contains a description of the Galaxy Zoo 2 (GZ2) sample data, which is used in the Bayesian statistics analysis of an exponentially declining star formation history model, all described in section 3. Section 4 contains the results produced by this analysis, with section 5 providing a detailing discussion of the results obtained. We also conclude our findings in section 6. The zero points of all ugriz magnitudes are in the AB system and where necessary we adopt the WMAP Seven-Year Cosmological parameters (Jarosik et al. , 2011) with $(\Omega_m, \Omega_\lambda, h) = (0.26, 0.73, 0.71)$.

2 DATA

See Galaxy Zoo 2 data release Willett et al. (2013).

WHERE does the data come from?

HOW do the users come into things?

HOW are the classifications made?

HOW do we get what we want from this?

WHAT can we do with it that's different?

WHY do we need it?

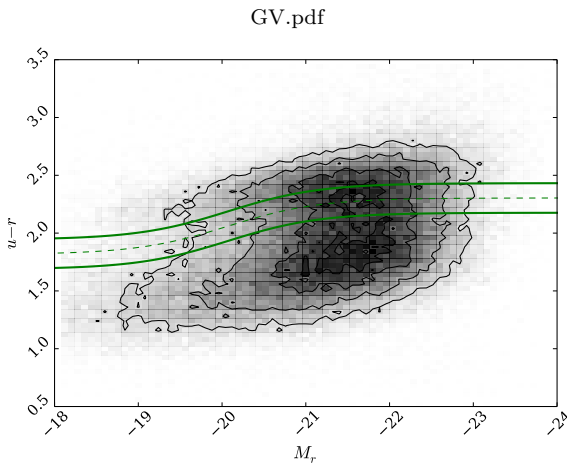


Figure 1. Colour-magnitude diagram for the GZ2 population showing the definition between the Blue Cloud and the Red Sequence from Baldry et al. (2004) with the dashed line. The solid lines show $\pm 1\sigma$ either side of this definition; any galaxy within the boundaries of these two solid lines is considered a Green Valley galaxy.

2.1 Defining the Green Valley

To define which of the GZ2 galaxies are in the Green Valley, we used the definition outlined in Baldry et al. (2004), which is shown in figure 1 by the dashed line. Anything within $\pm 1\sigma$ of this relationship, shown by the solid lines in figure 1, was considered a Green Valley galaxy. We decided upon a conservative Green Valley in order to remove any influence from tail galaxies from either the red sequence or blue cloud.

3 A BAYESIAN ANALYSIS

3.1 Stellar Population Synthesis Models

Using an assumed initial mass function (IMF), stellar population synthesis models (SPS) models calculate the total flux emitted by a population, as described in Bruzual & Charlot (2003)

3.2 Modelling the Star Formation History

We model the star formation history of a population with an exponentially declining star formation rate (SFR) at time steps from $t = 0 \text{ Gyr}$ to $t = 13.7 \text{ Gyr}$ as:

$$\text{SFR} = \begin{cases} c_{\text{SFR}} & \text{if } t < t_q \\ c_{\text{SFR}} \times \exp\left(\frac{-(t-t_q)}{\tau}\right) & \text{if } t > t_q \end{cases}$$

where t_q is the onset time of quenching, τ is the timescale over which the quenching occurs and c_{SFR} is a constant star formation rate. This constant star formation rate is set using Peng et al. (2010), who defined a relation (in their equation 1) between the average SFR and cosmic time as:

$$s\text{SFR}(m, t) = 2.5 \left(\frac{m}{10^{10} M_\odot} \right)^{-0.1} \left(\frac{t}{3.5} \right)^{-2.2} \text{Gyr}^{-1}$$

At the point of quenching, t_q , the models are defined to

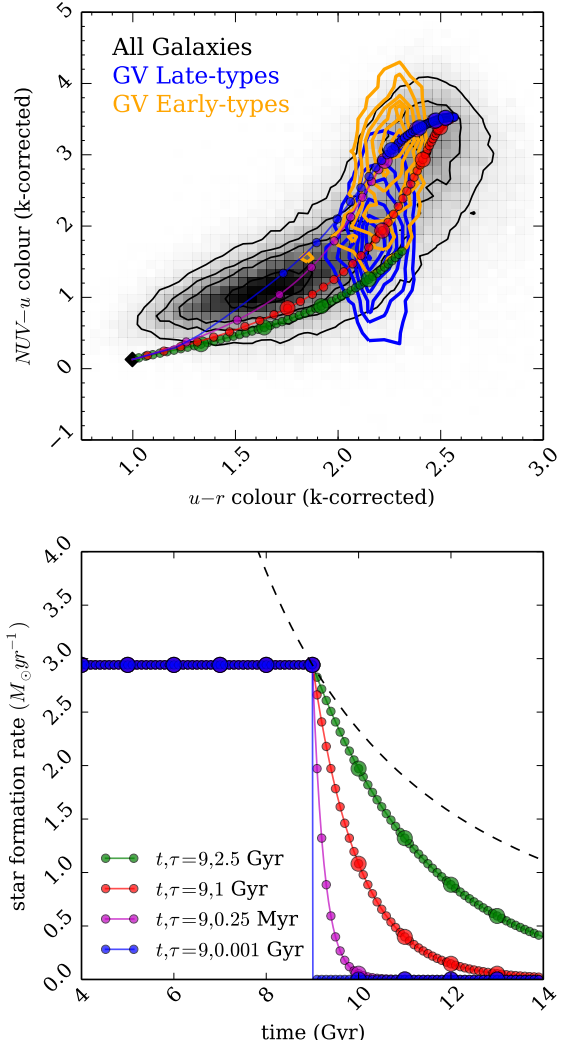


Figure 2. Exponentially declining star formation history models with $t_{\text{quench}} = 9 \text{ Gyr}$ and various τ values are shown in the bottom panel. The dashed line shows the average SFR with lookback time from Peng et al. (2010) which is used to set the c_{SFR} at t_{quench} (see section 3.2). The top panel shows the evolution with time (each point represents a time step of 1 Gyr) of these models across the optical-NUV colour-colour diagram. Also shown is the distribution of the GZ2 galaxies across this colour space by the black contours.

have a SFR which lies on this relationship for a galaxy with mass, $M = 10^{10.27} M_\odot$ the average mass of the GZ2 sample; see bottom panel of figure 2 and right panel of figure 3. Peng et al. (2010) state that beyond $z \sim 2$ the characteristic sSFR flattens and is roughly constant back to $z \sim 6$. The cause for this change is not well understood but can be seen across similar observational data (González et al. (2010) and Béthermin et al. (2012)). Motivated by these observations, we took the relation as defined in Peng et al. (2010) up to a cosmic time of $t = 3 \text{ Gyr}$ ($z \sim 2.3$) and prior to this assumed constant SFR, as shown by the dotted line in the right panel of figure 3.

We are aware that the average SFR of our models will result in a lower value than the relation defined in the Peng

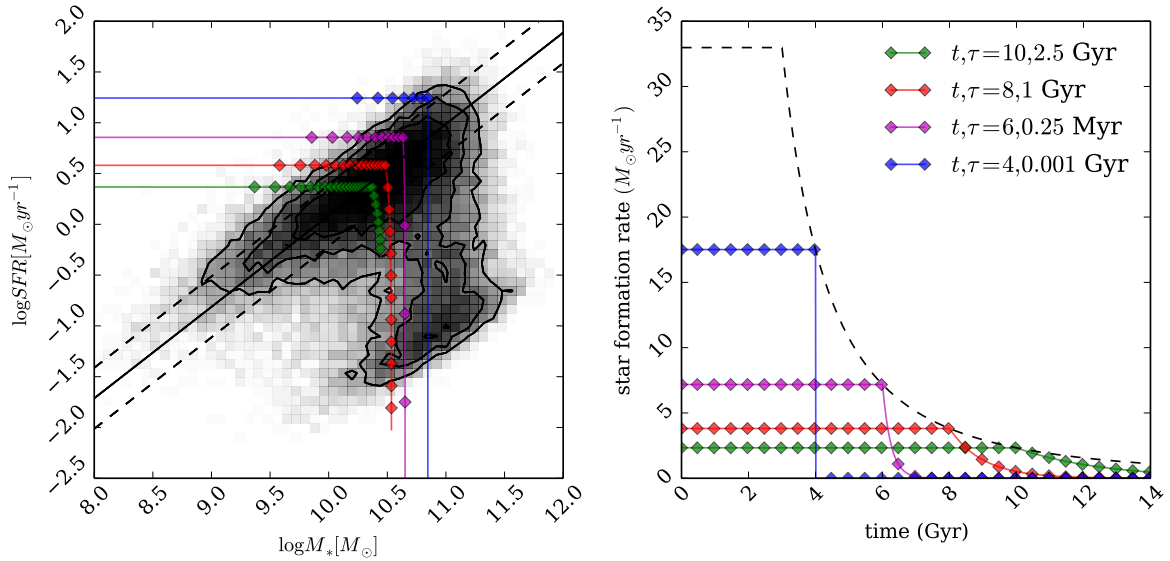


Figure 3. The right hand panel shows the relationship between the star formation rate and stellar mass for the galaxies in the GZ2 sample (black contours), which trace the "main sequence" of star formation (solid line from Peng et al. (2010) with ± 0.3 dex scatter shown by the dotted lines). The SFRs and masses of the model galaxies are also shown with corresponding star formation histories shown in the left hand panel. The dashed line in the left hand panel shows the relationship between the SFR and time as defined in equation 1 of Peng et al. (2010).

et al. (2010) relation at all cosmic times with this treatment, as each galaxy only resides on the 'main sequence' at the point of quenching. However, as Béthermin et al. (2012) points out, galaxies cannot remain on the 'main sequence' from early to late times throughout its lifetime given the resultant stellar masses and SFR they would then have at the current epoch in the local Universe. If we were to include prescriptions for galaxies which never undergo quenching or those with energetic starbursts into our models we would improve on our reproduction of the average SFR across cosmic time; however we have chosen to focus only on describing galaxies through a quenching model.

The left hand plot in figure 3 shows how well these models reproduce the observed relationship between the SFR and the mass of a galaxy, including how at the time of quenching they reside on the "main sequence" of star formation, shown by the solid black line for a galaxy of mass, $M = 10^{10.27} M_{\odot}$. We can also see in figure 4 how this diagram evolves with cosmic time according to our model predictions.

In our models a smaller τ value corresponds to a rapid quench (almost instantaneous suppression of star formation), whereas a large value of τ corresponds to a slower quench (slower than the dynamical timescale of a galaxy). This model assumes that all of the populations form an initial burst of stars at $t = 0$, the mass of which is set by the value of c_{SFR} .

Once this evolutionary SFR is obtained, we convolved it with the BC03 population synthesis models to generate a model SED for each time step. We suppress the fluxes from stars younger than 3 Myr to mimic the effect of birth clouds, then apply filter transmission curves to obtain AB magnitudes and therefore colours. How these colours evolve

in the optical-NUV colour space can be seen in the top panel of Figure 2.

We can "observe" these model stellar populations at a given time in their history; this correlates to the lookback time at which we observe them and therefore, if they were real populations, a measurable redshift (assuming all galaxies are formed at a time $t = 0$). Therefore, for each galaxy in the GZ2 sample, the lookback time was calculated from the redshift (using the *cosmology* package provided in the Python module *astroPy*) in order to compare the observed colours to the predicted models colours at that time. This lookback time t^{lb} can be thought of as a galaxy's age if we assume that all galaxies formed with an initial burst of star formation at $t = 0$.

Figure 5 shows the predicted optical and NUV colours at a time of $t^{lb} = 12.8 \text{ Gyr}$ (the average look back time of the Galaxy Zoo 2 sample) provided by the exponential SFH model. These predicted colours will be referred to as $d_p(t_q, \tau, t^{lb})$. The SFR at a time of $t^{lb} = 12.8 \text{ Gyr}$ is also shown in Figure 5 to compare how this correlates with the predicted colours. The $u - r$ predicted colour shows an immediate correlation with the SFR, however the $NUV - u$ colour is more sensitive to the value of τ and so is ideal for tracing any recent star formation in a population. At small τ (rapid quenching timescales) the $NUV - u$ colour is insensitive to t_q , whereas at large τ (slow quenching timescales) the colour is very sensitive to t_q . Together the two colours are ideal for tracing the effects of t_q and τ in a population.

3.3 Bayesian Analysis

In order to achieve robust conclusions we conducted a fully Bayesian analysis of our SFH models in comparison to the observed GZ2 sample data. To do this we must consider all

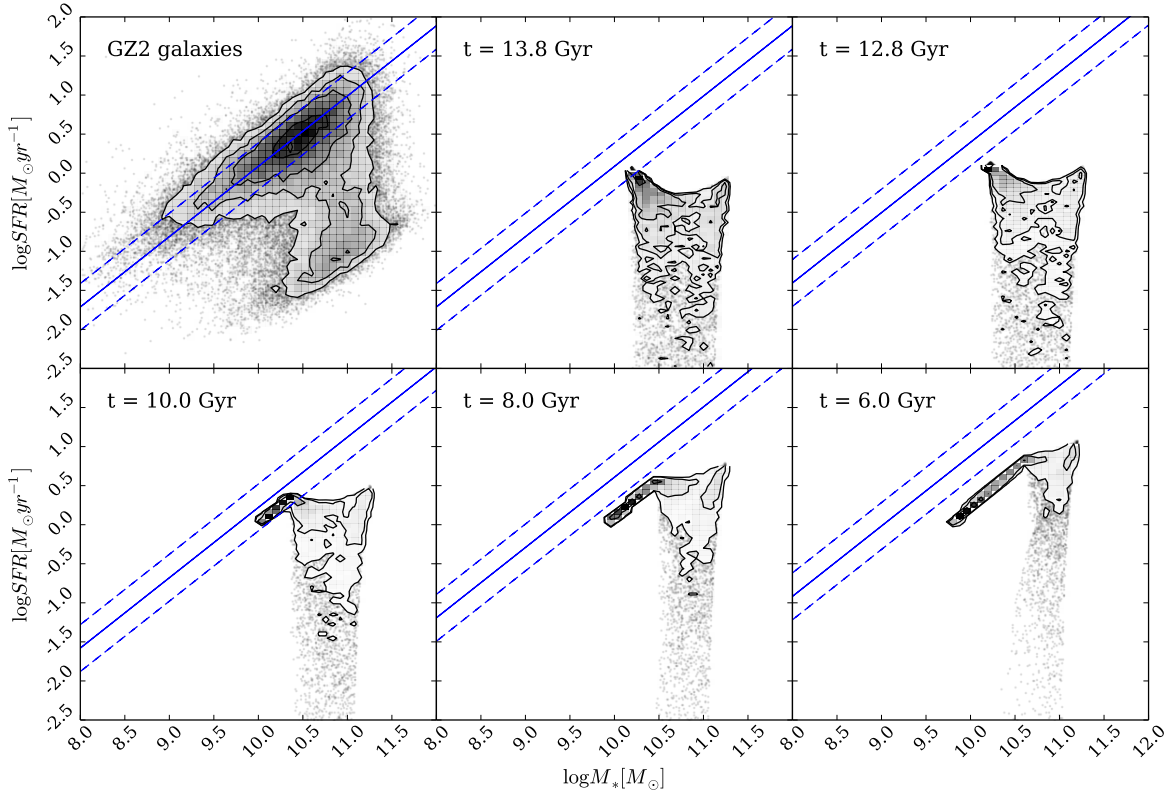


Figure 4. Plots to show the evolution of the SFR against the mass as predicted by the most likely exponential SFH model for each GZ2 galaxy. Each panel shows the models at different look-back times in the history of the Universe. The panel on the far left also includes the contours of the observed SFR against the mass of the GZ2 galaxies. Each panel also shows the ‘‘main sequence’’ of star formation as measured at the current epoch.

possible combinations of $(t_q, \tau) = \theta$ which will be distributed with a mean, μ and standard deviation, σ , so that:

$$w = (\mu_\theta, \sigma_\theta) = (\mu_{t_q}, \sigma_{t_q}, \mu_\tau, \sigma_\tau)$$

We can then define the Bayesian probability $P(\theta|w) = P(t_q, \tau|w) = P(t_q|w)P(\tau|w)$ assuming that $P(t_q|w)$ and $P(\tau|w)$ are independent of each other, so that:

$$\begin{aligned} P(t_q, \tau|w) &= \frac{1}{\sqrt{4\pi^2 \sigma_{t_q}^2 \sigma_\tau^2}} \exp \left[-\frac{(t_q - \mu_{t_q})^2}{2\sigma_{t_q}^2} \right] \\ &\quad \exp \left[-\frac{(\tau - \mu_\tau)^2}{2\sigma_\tau^2} \right]. \end{aligned}$$

This is equivalent to:

$$P(\theta|w) = \frac{1}{Z_\theta} \exp \left[-\frac{\chi_\theta^2}{2} \right].$$

Therefore if we work in logarithmic probabilities:

$$\log[P(\theta|w)] = -\log(Z_\theta) - \frac{\chi_\theta^2}{2}.$$

We must then find the probability of all of the GZ2 data (d) given a SFH model, i.e. a single combination of θ values, $P(\underline{d}|\theta, t_k^{lb})$:

$$P(\underline{d}|\theta, t_k^{lb}) = \prod_k P(d_k|\theta, t_k^{lb}),$$

where d_k is a single data point of one galaxy. Assuming that all galaxies formed at $t = 0$ Gyr with an initial burst of star formation, we can assume that the ‘age’ of each galaxy in the GZ2 sample is equivalent to its look-back time, t_k^{lb} , which can be calculated from its observed redshift. We then use this ‘age’ to calculate the predicted model colours at this cosmic time for a given combination of θ : $d_{c,p}(\theta, t_k^{lb})$ for both optical ($c = opt$) and NUV ($c = NUV$) colours. We can now directly compare our model colours with the observed GZ2 galaxy colours, so that $P(d_k|\theta, t_k^{lb})$:

$$\begin{aligned} P(d_k|\theta, t_k^{lb}) &= \frac{1}{\sqrt{2\pi\sigma_{opt,k}^2}} \frac{1}{\sqrt{2\pi\sigma_{NUV,k}^2}} \\ &\quad \exp \left[-\frac{(d_{opt,k} - d_{opt,p}(\theta, t_k^{lb}))^2}{\sigma_{opt,k}^2} \right] \\ &\quad \exp \left[-\frac{(d_{NUV,k} - d_{NUV,p}(\theta, t_k^{lb}))^2}{\sigma_{NUV,k}^2} \right], \end{aligned}$$

where for one combination of θ ,

$$\chi_{c,k}^2 = \frac{(d_{c,k} - d_{c,p}(\theta, t_k^{lb}))^2}{\sigma_{c,k}^2}$$

and

$$Z_k = \sqrt{2\pi\sigma_{c,k}^2}.$$

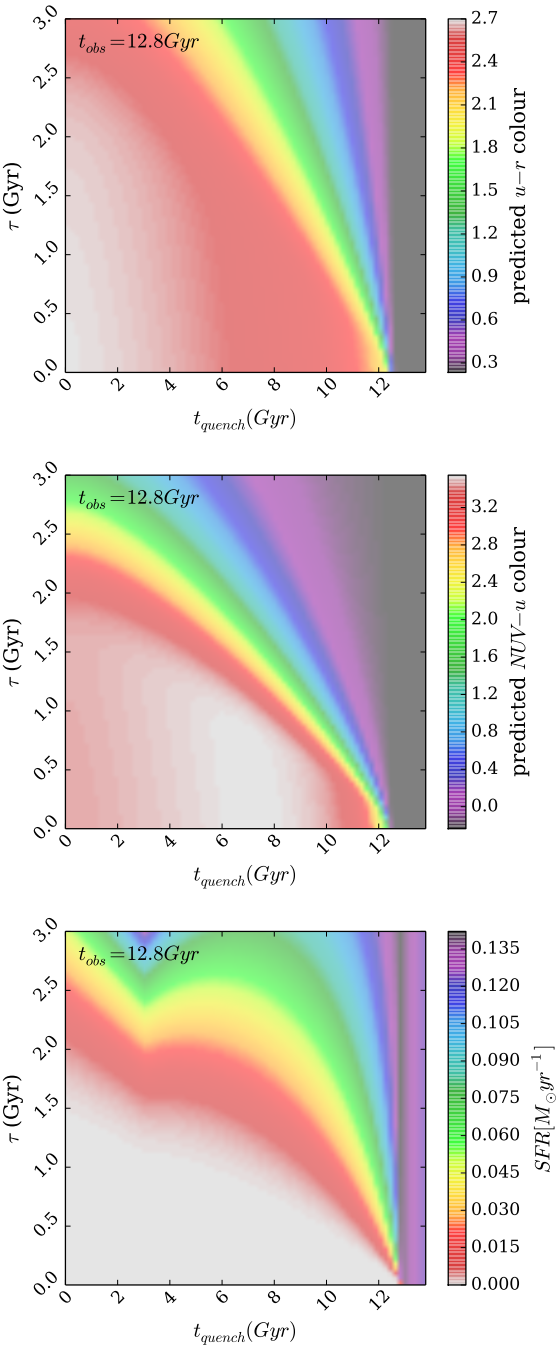


Figure 5. Model predictions of the $u - r$ and $NUV - u$ colours in the top and middle panels respectively when the population is observed at $t^{lb} = 12.8 \text{ Gyr}$ (the average look back time of the GZ2 sample, calculated from the observed redshifts). In the bottom panel, the SFR at a time of $t^{lb} = 12.8 \text{ Gyr}$ predicted by the models is shown. In all three plots, it can be seen that the models beyond $t > 12.8 \text{ Gyr}$ have not undergone any quenching, as they have been ‘observed’ before this time.

Again working in logarithmic probabilities:

$$\log(P(\underline{d}|\theta, t^{lb})) = \sum_{c,k} \log(P(d_{c,k}|\theta, t_k^{lb}))$$

$$\log(P(\underline{d}|\theta, t^{lb})) = K - \sum_{c,k} \frac{\chi_{c,k}^2}{2},$$

where K is a constant:

$$K = - \sum_{c,k} \log Z_{c,k},$$

where $c = \{opt, NUV\}$.

What we need however is the probability of each combination of θ values given the GZ2 data: $P(\theta|\underline{d})$, i.e. how likely is a single SFH model given the observed colours of all of the GZ2 galaxies. We can find this by:

$$P(\theta|\underline{d}) = \frac{P(\underline{d}|\theta, t^{lb})P(\theta|w)}{\int P(\underline{d}|\theta, t^{lb})P(\theta|w)d\theta},$$

where,

$$P(\underline{d}|\theta, t^{lb})P(\theta|w) = \exp \left[\log [P(\underline{d}|\theta, t^{lb})] + \log [P(\theta|w)] \right],$$

This denominator is a mere normalisation factor, therefore when we compare the likelihoods between two different SFH models, i.e. two different combinations of $\theta = (t_q, \tau)$ we need only compare the numerator and can also remain in logarithmic probability space. So, given the data from the GZ2 sample, we can calculate $\log[P(\theta|\underline{d}, t^{lb})]$ for all possible θ values and compare these to determine the most likely values for θ given the GZ2 data. In order to do this robustly, we performed a Markov Chain Monte Carlo (MCMC) sampling method to cycle through the defined parameter space using a Python implementation of an affine invariant ensemble sampler by Foreman-Mackey et al. (2013); *emcee*.

In addition to the colours, the GZ2 data is unique in that it provides information on a galaxy’s morphology. Vote fractions from GZ2 users are available for each galaxy, for example if 80 of 100 people thought a galaxy was disc shaped, whereas 20 out of 100 people thought the same galaxy was smooth in shape (i.e. elliptical), that galaxy would have $p_s = 0.2$ and $p_d = 0.8$. In this example this galaxy would be included in the ‘clean’ disc sample according to Willett et al. (2013). If we ran the above sampling method on galaxies in either of the *clean* samples, we lose all the information about the intermediate galaxies and how these contribute to the likelihood of $P(\theta|\underline{d})$. It is the intermediate galaxies which are thought to be crucial to the morphological changes between disc and elliptical galaxies; if this change is associated with the Green Valley in any way then these vote fractions are information we wish to keep in our sampling.

Instead we can incorporate these GZ2 vote fractions into our sampling by considering them as weightings to the likelihood $P(d_k|\theta)$ to which that galaxy contributes to $P(\underline{d}|\theta)$. For example a galaxy which has $p_s = 0.9$ should carry more weight in the likelihoods for the model parameters to describe smooth galaxies than a galaxy with $p_s = 0.1$. Therefore the likelihood can now be thought of as:

$$P(\underline{d}|\theta, t^{lb}) = \prod_k p_k P(d_k|\theta, t_k^{lb}),$$

where p_k is either p_s or p_d for a single galaxy, k . We can

then run the code with the GZ2 sample along with firstly, the p_s vote fractions to find the most likely parameters for θ for elliptical galaxies and secondly, with the p_d vote fractions to find the most likely parameters for θ for disc galaxies. However, this is costly in computing time, therefore we perform our sampling across four parameters so that $\theta = (t_s, \tau_s, t_d, \tau_d) = (\theta_s, \theta_d)$ and our likelihood function becomes:

$$P(\underline{d}|\theta, t^{lb}) = \prod_k \left[p_{s,k} P(d_k|\theta_s, t_k^{lb}) + p_{d,k} P(d_k|\theta_d, t_k^{lb}) \right],$$

or,

$$\log \left[P(\underline{d}|\theta, t^{lb}) \right] = \sum_k \log \left[p_{s,k} P(d_k|\theta_s, t_k^{lb}) + p_{d,k} P(d_k|\theta_d, t_k^{lb}) \right].$$

The MCMC algorithm searches through the θ parameter space to find the region that maximises $P(\underline{d}|\theta)$ to return four parameter values for t_s, τ_s, t_d and τ_d . If we find that $t_s \sim t_d$ and $\tau_s \sim \tau_d$ for the Green Valley galaxies then we can conclude that this area of the colour-magnitude diagram consists of single population that have a shared star formation history. The statistics outlined above have been coded using the *Python* programming language into a package named: *StarfPy* which has been made freely available to download.

4 RESULTS

The contour plots in figure 6 show the regions of high likelihood for the SFH model parameters $\theta = (t, \tau)$ for both smooth- and disc-like galaxies (left and right panels respectively) when considering all of the galaxies in the GZ2 sample. These plots were produced by *StarfPy* using the output of the MCMC sampling method outlined in section 3.3. The histograms show the distribution for the individual parameters and the colours in the background are provided as a reference to the predicted SFR at the average look-back time of the GZ2 sample ($t^{lb} = 12.8 \text{ Gyr}$, see figure 5).

We also consider how these areas of highest likelihood for each parameter changes when we consider different subsets of the GZ2 galaxy sample.

It is expected that those subsets of galaxies with large numbers will rapidly converge the ‘walkers’ into the regions of high likelihood without the need to explore the whole parameter space. Conversely the smaller galaxy subsets will allow a full exploration of the parameter space. It is also expected that those subsets of galaxies with narrow ranges of either NUV or optical colours will also cause the ‘walkers’ to converge rapidly into the regions of high likelihood without the need to explore the whole of the parameter space.

This raises the issue of whether the sampling method is capable of finding multiple likelihood peaks, however the figures in this section show that x is capable of finding multiple peaks in both parameters.

5 DISCUSSION

In figure 6 we can immediately see that the two populations occupy very different locations in the θ parameter space supporting the conclusion in Schawinski et al. (2014) that early- and late-type galaxies quench on different timescales. We

can also see a significant *correlation* between the two parameters t and τ (if quenching occurs earlier, then the quenching timescale increases) particularly for the disc-like galaxies. Perhaps this is due to a dependency on the environment which galaxies occupied at earlier times compared to later times.

For the disc-like galaxies we have a bimodal likelihood in the SFH parameter space, whereas for the smooth-like galaxies we have a trimodal likelihood. For the disc galaxies we see no likelihood below $\tau \sim 1 \text{ Gyr}$ (rapid quenching), whereas we do see an area of likelihood for the smooth galaxies - most likely caused by typical ‘red and dead’ early type galaxies. The areas of high likelihood for t for the disc-like galaxies spans a much larger range than for the smooth-like galaxies.

In figure 7 we can see those galaxies which are defined to be in the optical Red Sequence, show a prevalence for fast quenching timescales for the smooth-like galaxies and slow quenching timescales for the disc-like galaxies; again confirming the results found by Schawinski et al. (2014). However there is also a significant likelihood for blue NUV colours in the smooth parameters (slow quenching at late timescales) and for red NUV colours in the disc parameters. Could this be due to:

- (i) a population of S0 galaxies (with GZ2 likelihoods $p_s \sim p_d \sim 0.5$) which contribute to both sets of parameters?
- (ii) bulge dominated disc galaxies impacting on the likely disc parameters?
- (iii) NUV blue smooth galaxies impacting on the likely smooth parameters?

In figure 8 we try to remove the influence from these intermediate galaxies; the figure shows the SFH parameters but only for those galaxies defined to be both in the optical Red Sequence and the GZ2 ‘clean’ sample (i.e. $p_d \geq 0.8$ and $p_s \geq 0.8$). This enables us to disentangle which galaxies are contributing to which areas of high likelihood in figure 7. We can therefore see that the typical clean, smooth, red sequence galaxy has undergone a SFH with a relatively rapid quench at various early times, resulting in a very low current SFR. These are therefore the typical ‘red and dead’ galaxies expected to be found in the red sequence.

However for the clean disc galaxies in the red sequence (presumably the red spiral galaxies) there is no region of the parameter space which has a preferred higher likelihood, suggesting that although these disc galaxies are optically red, they have a wide range of NUV-u colours, giving rise to a wide range of timescales for the most recent episode of star formation. Although we can pick out a similar region of high likelihood as seen for smooth galaxies in the left panel of figure 8, we can see a preference for high likelihood across all regions of the parameter space. This suggests that there is no ‘typical’ red sequence disc galaxy and that there are many possible routes for a disc galaxy to the red sequence.

In figures 9 and 10 we can make similar comparisons as for the red sequence galaxies but now for the green valley galaxies. In figure 9 we still see the correlation between the two parameters as seen in figure 6 but the areas of high likelihood for the parameters has changed. We have a very clear bimodal likelihood in the parameter space for smooth galaxies; which is also slightly apparent in the likelihoods for the parameters for the disc-like green valley galaxies.

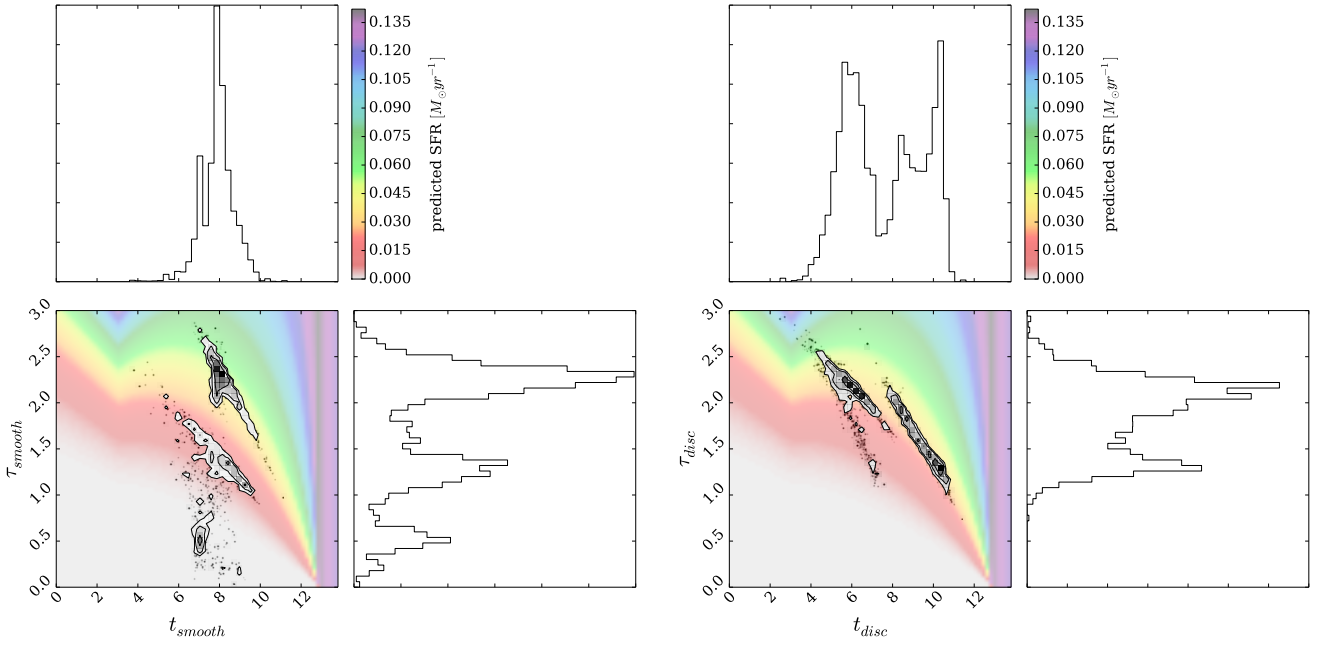


Figure 6. For all the galaxies in the Galaxy Zoo 2 sample, contour and histogram plots show the regions of greatest likelihood for an exponential model star formation history parameters [t_{quench} and τ_{quench}] for both smooth-like(left) and disc-like (right) galaxies. t_q is the time at which quenching occurs (Gyr) and τ_q is the time scale on which quenching occurs (Gyr; the larger the τ_q , the slower the quenching). Background colours show the star formation rate predicted by this model after a time $t \sim 12.8$ Gyr, which is the mean look back time of the galaxies in the GZ2 sample. Galaxies contribute to $[t_q, \tau_q]_{smooth}$ and $[t_q, \tau_q]_{disc}$ according to their Galaxy Zoo 2 vote fraction (i.e. a galaxy with $p_{disc} \sim p_{smooth} \sim 0.5$ will contribute equally to each set of parameters).

We can also see that quenching for the Green Valley occurs on longer quenching timescales; there is little to no likelihood for τ below ~ 1.0 Gyr for either the smooth- or disc-like galaxies, unlike in the previous plots. However there is a small likelihood for recent rapid quenching of the smooth galaxies. This may be counter intuitive at first, as one of the main arguments for the lack of galaxies in the green valley is due to the hypothesised rapid movement across it; however, if this is the case then the expected number of galaxies in this region with a very rapidly quenched SFH is very small.

It is remarkable therefore that we have managed to find a preference for this type of SFH in the parameter space (as seen in the left hand panel of figure 9). This is only apparent for the smooth-like galaxies, suggesting that it is only early-type galaxies which traverse the green valley in this rapid fashion. Conversely the disc galaxies come to reside in the green valley after a relatively slow quench causing a transition from the centre of the blue cloud to the edge and eventually into the green valley. Given enough time with this slow decline of star formation these galaxies may also make it to the edge of the red sequence, fully passing through the green valley. This is most likely the origin of the ‘red spirals’ and explains why there are currently so relatively few of them.

If we compare figure 9 to figure 10, which shows the regions of high likelihood for the model parameters for only the ‘clean’ green valley galaxies, we can see that this bimodality has disappeared for both the smooth- and disc-like populations. This suggests that there are not just two routes for galaxies through the green valley but *three*: with the smooth, intermediate (e.g. S0 galaxies) and disc galax-

ies each having different SFHs which eventually lead them across the Green Valley.

In figure 11 there is a preference for slow quenching at late times for both smooth- and disc-like galaxies but in this case we see a bimodality (or trimodality) in both populations, which is more pronounced in the disc galaxies, compared to figure 6. Both sets of parameters show high likelihood for slow quenching at late times, which is not unexpected; typically the blue cloud will consist of galaxies whose SFH consisted of no quenching to date. Again, as expected this has a higher likelihood for the disc-like galaxies.

There is also high likelihood in both samples for medium rate quenching at relatively recent times which could account for those galaxies on the edge of the blue cloud which have begun to quench. The SFH parameter space for the smooth-like and disc-like galaxies appear very similar, suggesting so too are galaxies in the blue cloud, irrespective of their morphology. Of all of the regions of the CMD, this is to be expected in the blue cloud since it consists of galaxies that are mostly still star forming, which this model does not account for. The way these galaxies differ is the mechanisms and triggers by which they have formed their stars, having no effect on the observed colours but a discernible effect on their morphologies.

This is apparent when we compare figures 11 and 12 which shows the likely model parameters for the ‘clean’ blue cloud galaxies. Now, the smooth galaxies only have high likelihood for a slow quench model at late times, suggesting that most of the obviously smooth blue galaxies in the GZ2 sample still have recent star formation occurring. Perhaps as their star formation begins to cease their morphology is

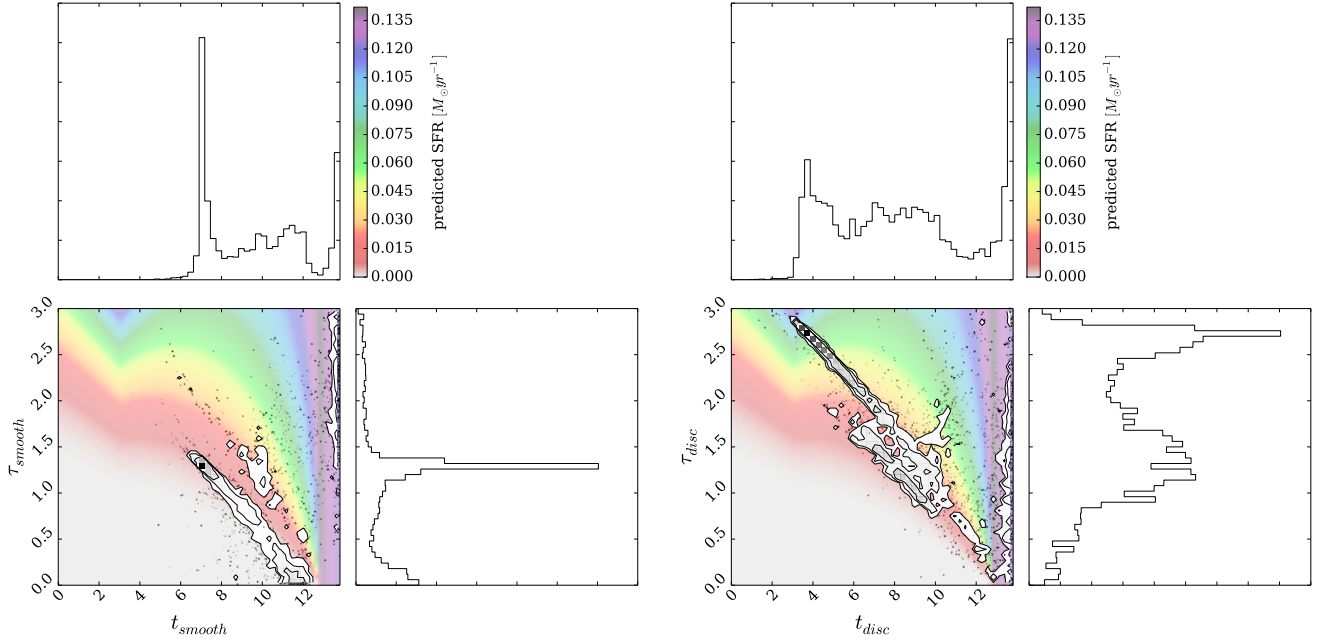


Figure 7. Same as for Figure 6 but for galaxies defined as optical Red Sequence Baldry et al. (2004).

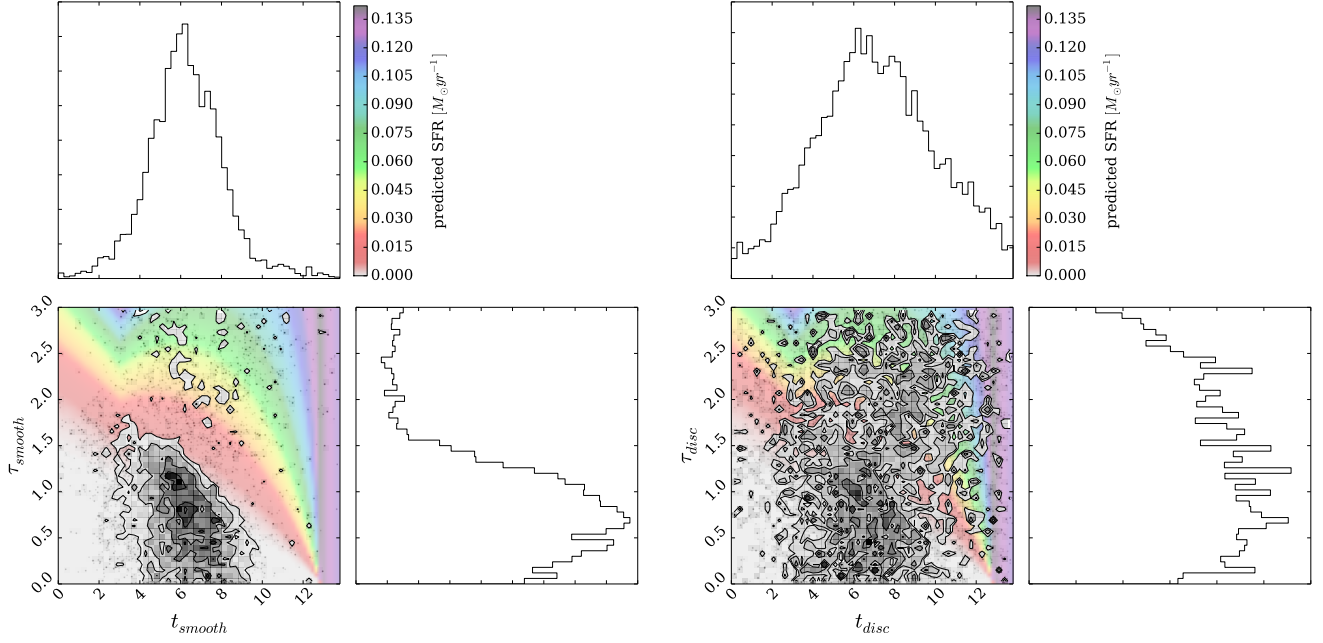


Figure 8. Same as for Figure 6 but for galaxies from the clean sample and defined as optical Red Sequence Baldry et al. (2004).

not as pronounced; does a lack of star formation in a galaxy relax the rigidity on its morphology?

The disc-like galaxies in the right panel of figure 12 show a high likelihood for any timescale of quenching at late times, which again is most likely indicative of very recent star formation having occurred or still occurring. We still keep however some preference for medium quenching at recent (late) times, suggesting that the edge of the blue

cloud is made primarily of disc-like galaxies rather than the smooth-like galaxies.

In figure 13 we can compare the star formation history parameters for barred and unbarred galaxies, selected so that $N_{count,bar} > 10$ and $N_{count,nobar} > 10$. The analysis was then run with p_{bar} and p_{nobar} in place of p_{smooth} and p_{disc} in the final equation in section 3.3. We can see that two the populations occupy different areas in the SFH parameter space suggesting that bars have indeed undergone a different

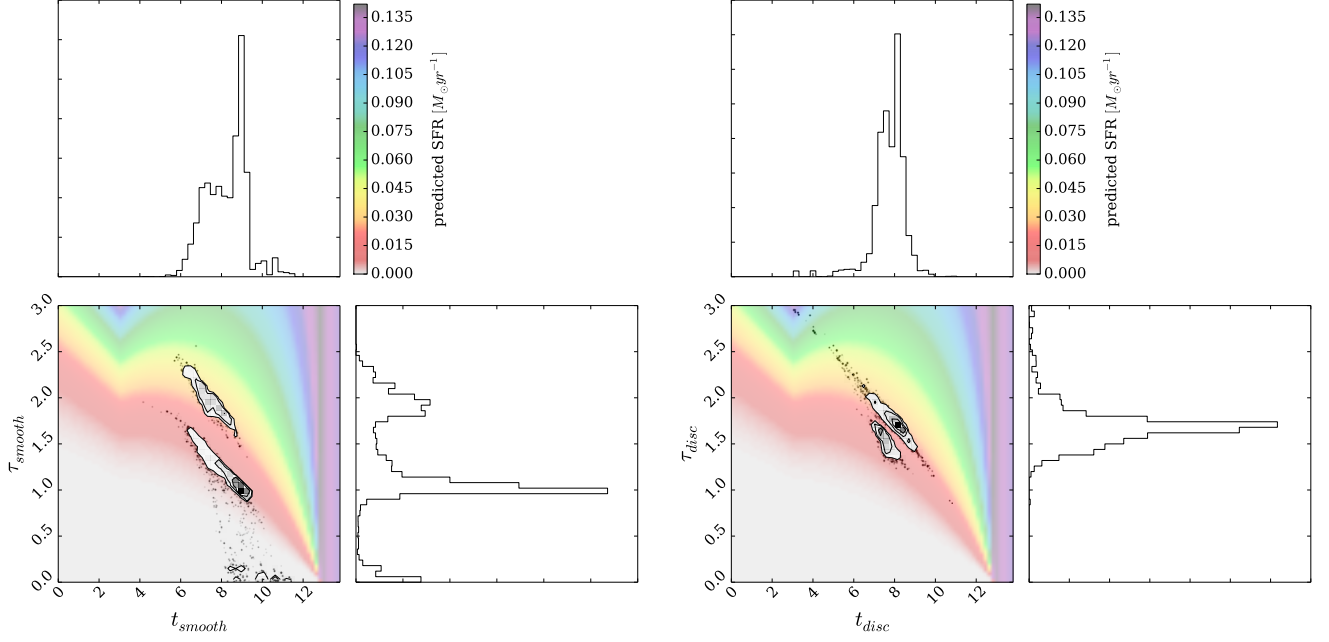


Figure 9. Same as for Figure 6 but for galaxies defined as optical Green Valley Baldry et al. (2004).

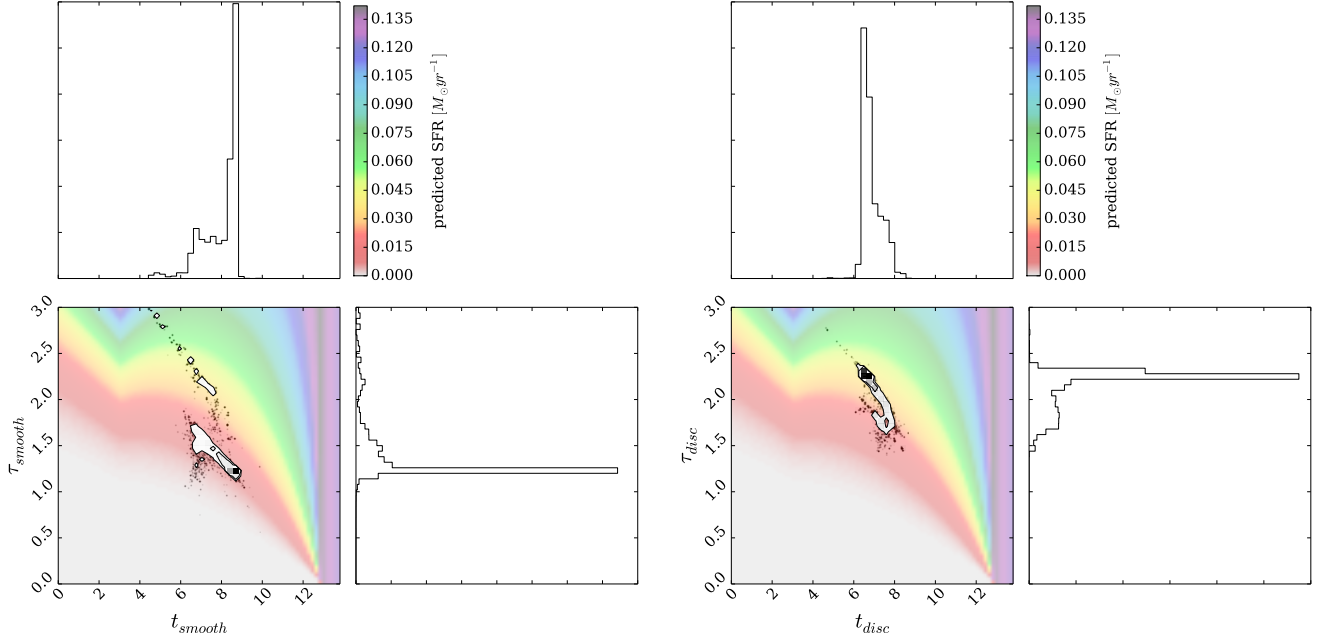


Figure 10. Same as for Figure 6 but for galaxies from the clean sample and defined as optical Green Valley Baldry et al. (2004).

formation history to non barred disc galaxies. Barred galaxies simultaneously are more likely to have both bluer and redder colours than non barred galaxies, as the bimodality seen in the SFH parameters of the non barred galaxies in the right hand panel of figure 13 has moved apart.

This suggests that the argument for whether bars promote or quench star formation rates in galaxies could have evidence for both possibilities. Perhaps the amount and distribution of gas present in a galaxy prior to the formation

of the bar determines what effect the bar will have on the star formation rate. There is also a region of likelihood at very rapid quenching timescales for barred galaxies which is not present in the parameters for the non barred galaxies, supporting the hypothesis that bars turn galaxies red (*cite Maraston papers here*). To explain what we see here we can say either that:

- (i) As a bar forms it can cause a rapid quenching of star formation in its host galaxy,

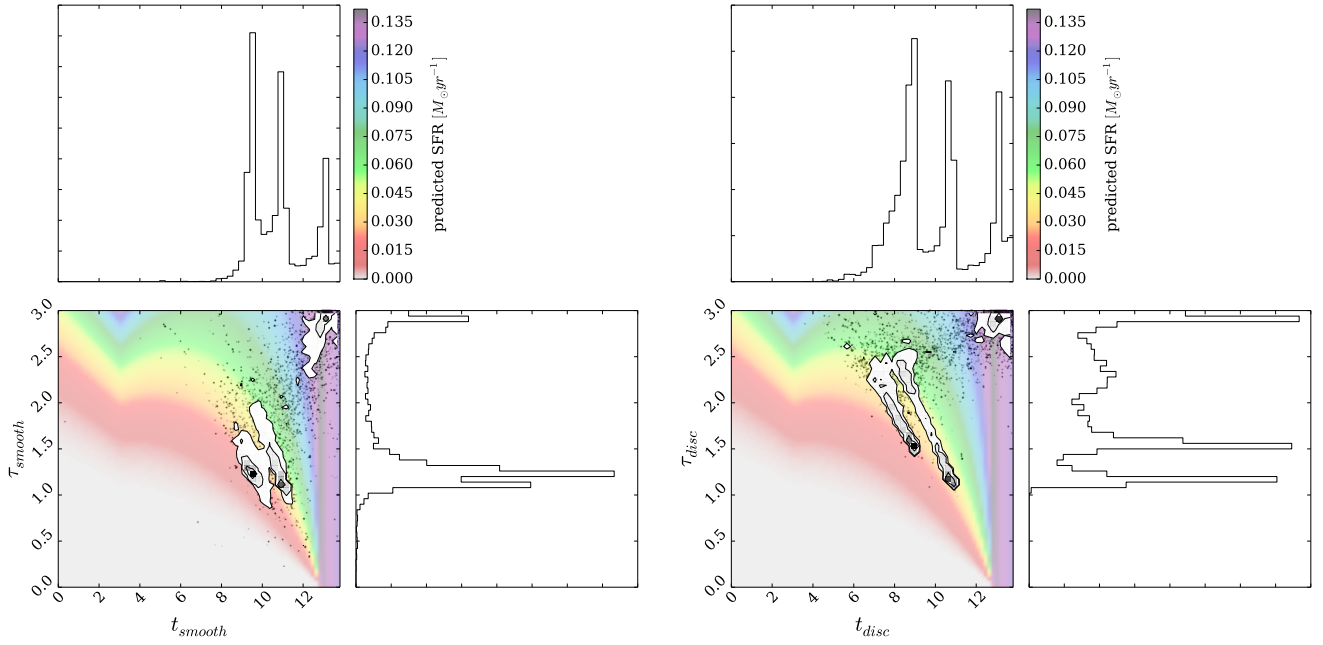


Figure 11. Same as for Figure 6 but for galaxies defined as optical Blue Cloud Baldry et al. (2004).

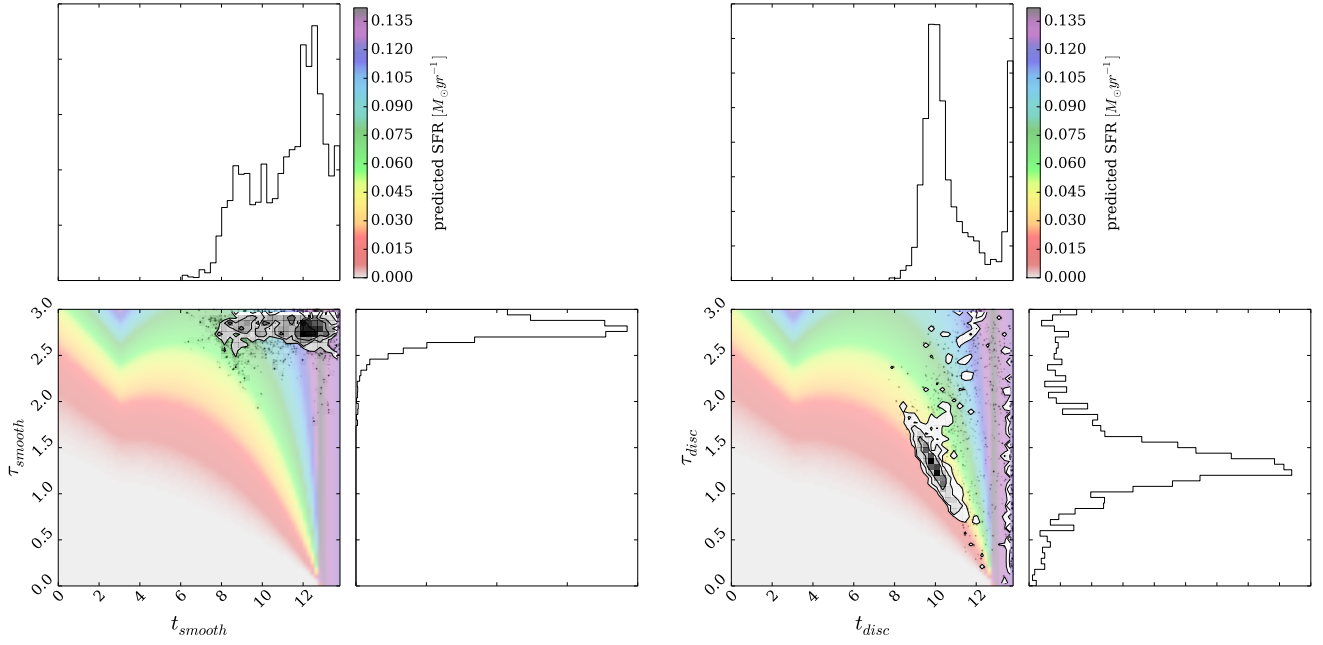


Figure 12. Same as for Figure 6 but for galaxies from the clean sample and defined as optical Blue Cloud Baldry et al. (2004).

(ii) A rapid quenching of star formation in a galaxy can cause a bar to form.

This analysis however, does not allow for this to be determined.

6 CONCLUSION

The three most important points:

(i) There is a clear correlation between t_{quench} and τ . At earlier times, the quenching timescale is longer, whereas at more recent times, the quenching timescale is shorter on average. Could this be an environmental dependence of quenching with cosmic time?

(ii) There are a wide range of possible routes to the red sequence for disc galaxies. Some have similar SFHs to the red sequence smooth galaxies, whereas some have similar

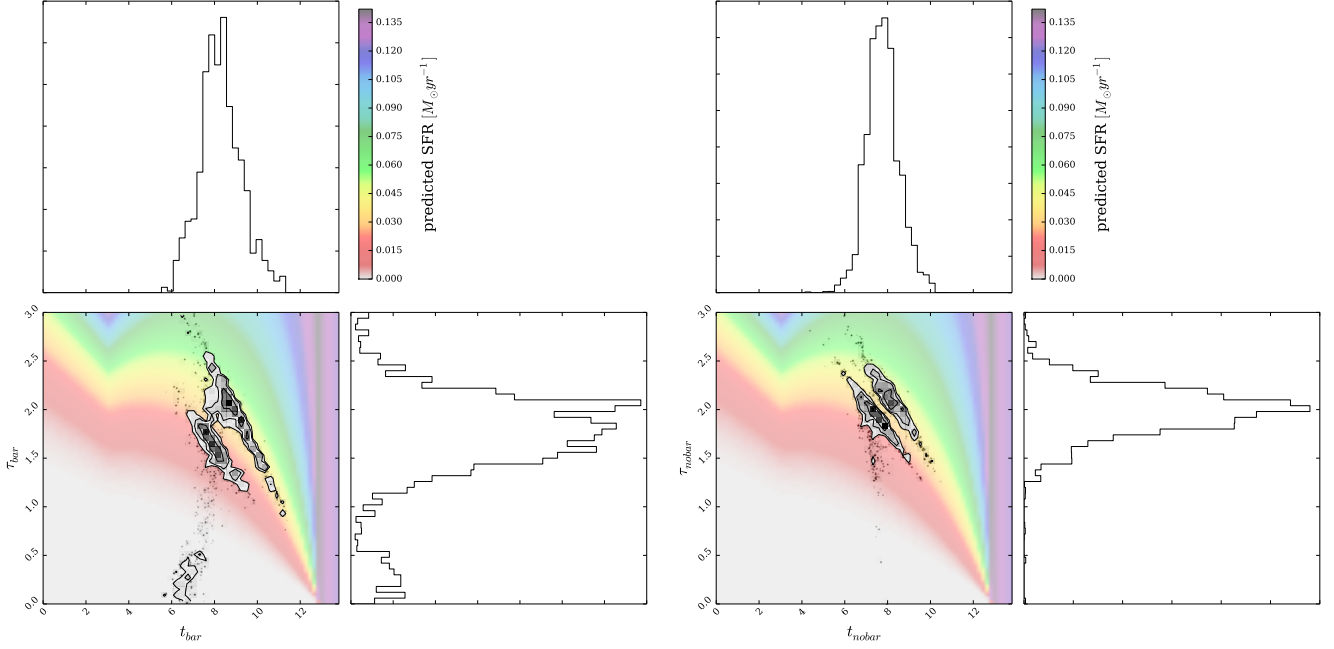


Figure 13. Same as for Figure 6 but for barred and non barred galaxies.

SFHs to blue cloud disc galaxies. Morphology seems to be irrelevant to the SFH.

(iii) There are three possible routes through the green valley dependant on morphology (smooth-like, intermediate and disc-like galaxies).

There is not one specific route to each part of the colour-colour or colour-magnitude diagram, due to the complex interplay between the SFH parameters, however the morphology of a galaxy can have varying impacts and constraints on what these parameters can be.

References

- Baldry, I. K. et al., 2004, ApJ, 600, 681
- Béthermin, M. et al., 2012, ApJ, 757, L23
- Bruzual, G. & Charlot, S., 2003, MNRAS, 344, 1000
- Foreman-Mackey, D., Hogg, D. W., Lang, D., Goodman, J., 2013, PASP, 125, 306
- González, V. et al., 2010, ApJ, 713, 115
- Jarosik, N. et al., 2011, ApJSS, 192, 18
- Peng, Y. et al., 2010, ApJ, 721, 193
- Schawinski, K. et al., 2014 (arXiv: 1402.4814)
- Willett, K. et al., 2014, MNRAS, 435, 2835